Provided for non-commercial research and education use.
Not for reproduction, distribution or commercial use.

This article appeared in a journal published by Elsevier. The attached copy is furnished to the author for internal non-commercial research and education use, including for instruction at the authors institution and sharing with colleagues.

Other uses, including reproduction and distribution, or selling or licensing copies, or posting to personal, institutional or third party websites are prohibited.

In most cases authors are permitted to post their version of the article (e.g. in Word or Tex form) to their personal website or institutional repository. Authors requiring further information regarding Elsevier's archiving and manuscript policies are encouraged to visit:

http://www.elsevier.com/copyright

Author's personal copy

Applied Surface Science 255 (2009) 7121–7125

Contents lists available at ScienceDirect

Applied Surface Science

journal homepage: www.elsevier.com/locate/apsusc

Passivation of GaSb and InAs by pH-activated thioacetamide

R. Stine [a], E.H. Aifer [a], L.J. Whitman [a,1], D.Y. Petrovykh [a,b,*]

[a] *Naval Research Laboratory, Washington, DC 20375, USA*
[b] *Department of Physics, University of Maryland, College Park, MD 20742, USA*

ARTICLE INFO

Article history:
Received 18 July 2008
Received in revised form 6 February 2009
Accepted 7 March 2009
Available online 17 March 2009

PACS:
81.05.Ea
81.65.Rv
81.65.Mq
79.60.Dp
82.80.Pv

Keywords:
X-ray photoelectron spectroscopy
Gallium antimonide
Indium arsenide
Thioacetamide
Passivation
Oxidation

ABSTRACT

We describe the passivation by thioacetamide (TAM) of GaSb and InAs—two III–V semiconductor materials important for fabricating IR devices from Type-II superlattices (T2SLs). We use X-ray photoelectron spectroscopy (XPS) to characterize GaSb and InAs (001) surfaces treated by TAM under both acidic and basic conditions and to analyze the reoxidation of passivated surfaces over time. Both acid- and base-activated TAM treatments produce sulfide layers on GaSb and InAs. The layers produced by base-TAM appear to be of self-limited thickness <1 nm, whereas acid-TAM creates considerably thicker (1–2 nm) sulfide layers. Passivation by both acid- and base-activated TAM offers significant short-term (<1 day) protection against reoxidation, but does not prevent oxide formation after exposure to ambient air for 1–3 days. Based on this comparative study and previous literature reports, the chemical effects of TAM treatments on Ga, Sb, In, and As depend not only on the individual element and reaction conditions, but also on the compound. In other words, our results suggest that passivation chemistry for a common element in two different III–V materials should not, in general, be assumed to be the same.

© 2009 Elsevier B.V. All rights reserved.

1. Introduction

We compare the effects of thioacetamide treatments on GaSb and InAs in order to bridge the gap between the fundamental studies of sulfur passivation of III–V materials and the application of methods derived from such studies to passivation of devices. Most published accounts focus on the effects of passivation on device performance without attempting to directly characterize the chemistry of the passivated surface [1–7]. As a result, surprisingly little is known about the chemical effects of various passivation treatments, despite the widespread research on the effects of passivation on performance of III–V devices.

The choice of *two* III–V semiconductors for our study helps to demonstrate another important aspect of applying chemical treatments to device structures. In devices, III–V materials typically are not used separately and independently, but rather as alternating layers in superlattices. For example, Type-II superlattices (T2SLs) of InAs and GaSb are emerging as a promising material system for mid- and long-wavelength IR LEDs [8] and photodetectors [1–5,7,9–14]. In these IR detectors, doped T2SLs are etched through the junction to produce an array of mesa-isolated photodiodes [3,4]; i.e., *both* superlattice materials are exposed to the ambient surroundings in these devices. Therefore, the effects of each passivation method on *both* InAs and GaSb surfaces must be analyzed to fully understand and optimize device passivation.

In unpassivated InAs/GaSb T2SLs, the high surface recombination velocity on the exposed sidewalls of mesa photodiodes results in excess dark current [3,4]. Theoretically, InAs/GaSb T2SLs provide tunable and strong optical absorption, a narrow-gap band structure, large effective masses, and low Auger recombination rates. Therefore, compared with HgCdTe (MCT) devices, effectively passivated T2SLs should be able to operate at higher temperatures.

Sulfur passivation has been used effectively to passivate exposed surfaces of III–V semiconductor devices [15–25], and has been previously attempted for T2SLs [2–4,7]. Historically, most common sulfur passivation treatments have been performed in aqueous solutions of inorganic sulfides, such as $(NH_4)_2S_x$ [16,17,23,26–28] or Na_2S [18,26,27,29]. More recently, an alternative treatment based on thioacetamide (TAM), an organic sulfide, has been proposed and its effectiveness examined in some

* Corresponding author. Tel.: +1 202 404 3381; fax: +1 202 767 3321.
E-mail address: dmitri.petrovykh@nrl.navy.mil (D.Y. Petrovykh).
[1] Current address: Center for Nanoscale Science and Technology, National Institute of Standards and Technology, Gaithersburg, MD 20899, USA.

0169-4332/$ – see front matter © 2009 Elsevier B.V. All rights reserved.
doi:10.1016/j.apsusc.2009.03.010

Author's personal copy

detail [6,7,21,22,24,25]. Surface passivation by TAM compares favorably to that by inorganic sulfides [25] and offers advantages such as milder reaction conditions and the ability to passivate under both acidic and basic conditions. Here, we use X-ray photoelectron spectroscopy (XPS) to characterize GaSb and InAs surfaces passivated by TAM under acidic ("acid-TAM") and basic ("base-TAM") conditions, and to analyze the extent of reoxidation of the passivated surfaces over time.

2. Experimental details

Homoepitaxial GaSb(001) and InAs(001) 0.5 μm-thick undoped epilayers were grown on 5 cm-diameter epi-ready substrates (Wafer Technology Ltd., U.K.) by solid-source molecular beam epitaxy in a Riber compact 21T system equipped with valved arsenic and antimony crackers. The "acid-TAM" or "base-TAM" solutions were prepared by dissolving thioacetamide powder (CH_3CSNH_2, 99.0%, ACS reagent grade) in, respectively, glacial acetic acid (Fisher Scientific), or ammonium hydroxide (29.7% stock solution, Fisher Scientific), diluted 1:10 by volume in deionized water.

In this paper, samples treated by TAM solutions are referred to as "passivated" and compared to "unpassivated" and "untreated" controls. *Passivated* samples were placed for 40 min in 0.18 M TAM solutions (at acidic or basic pH, as described above) held at 70 °C in a water bath. After treatment, samples were rinsed in copious amounts of deionized water, dried with flowing nitrogen, and maintained under ambient atmospheric conditions between XPS measurements. *Unpassivated* control samples were stripped of their native oxide films using AZ400K (Clariant Corporation, Somerville, NJ) for GaSb and 15% NH_4OH for InAs. *Untreated* control samples were as-grown GaSb and InAs films exposed to ambient air for a specified time.

XPS characterization was performed in a commercial XPS system equipped with a monochromatic Al Kα source, a magnetic lens, and a hemispherical electron energy analyzer [24]. The high-resolution data (nominal analyzer resolution of 0.36 eV) were acquired in angle-integrated normal emission mode and quantitatively analyzed following a previously described procedure [24]. Surface roughness was measured using an atomic force microscope (AFM) operated in contact mode.

3. Results and discussion

3.1. Freshly-passivated surfaces

We find that III–V surfaces treated by TAM solutions at different pH exhibit dramatically different chemistries, as evidenced by XPS data for freshly-passivated GaSb (Fig. 1(b)) and InAs (Fig. 1(c)). The corresponding bulk, sulfide, and oxide components for each element (Table 1) can be identified and quantified by fitting the high-resolution spectra in Fig. 1 [24,30]. A basic TAM solution (spectra marked "base-TAM" in Fig. 1) produces self-limiting thin layers composed primarily of sulfides on both GaSb and InAs. The resulting sulfide components (shaded gray in Fig. 1) are both element- and compound-dependent, with about twice as much Sb–S as Ga–S on GaSb (Fig. 1(b)) and almost exclusively In–S on InAs (Fig. 1(c)).

Compared to base-TAM, acid-TAM solutions create considerably thicker sulfide layers on GaSb [note the increased sulfide and suppressed bulk components in both Ga and Sb spectra in Fig. 1(b)]. On InAs, roughly the same amount of In–S is formed under acidic and basic conditions, but in acid-TAM there is appreciable As–S formation, approximately 50% higher than the amount of In–S (Fig. 2(b)). The surface termination after acid-TAM treatment, therefore, is a mixture of As–S and In–S, in

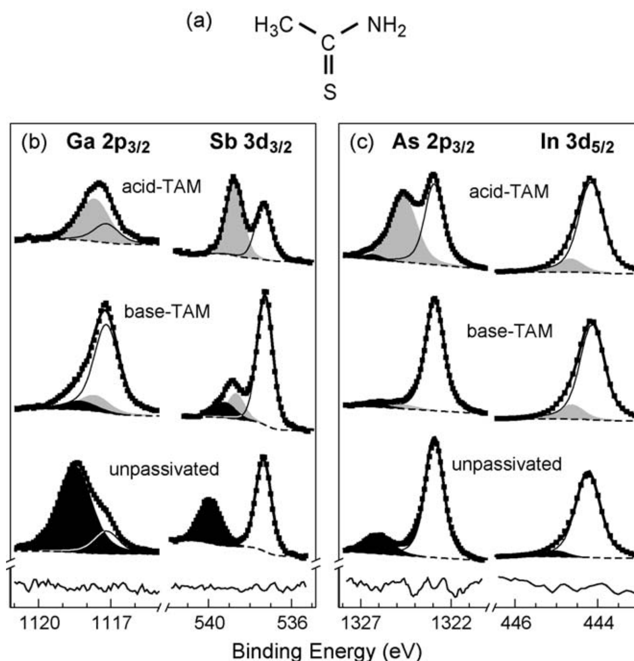

Fig. 1. XPS data for TAM-treated GaSb and InAs samples. Solutions of TAM (a) activated with acid or base were used to passivate GaSb (b) and InAs (c) samples; unpassivated controls were treated only to remove native oxides. Exposure to ambient air before XPS measurements was ≤5 min. Indicated in fits for each element are bulk (thin line, no shading), sulfide (gray shading), and oxide (black shading) chemical components (Table 1). Symbols = data points; thick lines = overall fits; dashed lines = backgrounds; representative fit residuals are shown at the bottom of panels. The minority-spin Sb $3d_{3/2}$ component was used for peak fits in (b) to avoid overlap with O 1s.

Table 1
XPS peak fitting parameters for TAM-treated InAs and GaSb samples.

Peak	Component	BE (eV)	FWHM (eV)		Intensity ratio vs. bulk	
			Lorentzian	Gaussian	Acid-TAM	Base-TAM
In $3d_{5/2}$	In–As	444.2	0.32	0.51	–	–
	In–S	444.7	0.32	0.51	0.15	0.15
	In–O	445.0	0.32	1.2	0	0.007
As $2p_{3/2}$	As–In	1323.0	0.50	0.94	–	–
	As–S	1324.7	0.50	1.5	1.1	0.05
	As–O	1326.2	0.50	1.5	0.06	0.03
Ga $2p_{3/2}$	Ga–Sb	1117.2	0.66	0.83	–	–
	Ga–S	1117.7	0.66	1.1	2.7	0.21
	Ga–O	1118.3	0.66	1.2	0	0.12
Sb $3d_{3/2}$	Sb–Ga	537.3	0.15	0.82	–	–
	Sb–S	538.7	0.15	0.88	1.4	0.27
	Sb–O	539.9	0.15	1.2	0	0.12

contrast to the exclusive In–S termination that we have observed after base-TAM treatment, both here and previously [24,25]. We note that both acid- and base-TAM-treated surfaces are relatively smooth (≈4 Å RMS roughness over a 1 μm^2 area), suggesting that there is not a significant differential etch rate under these conditions.

In analyzing the XPS results for the GaSb samples, the spin-orbit minority Sb $3d_{3/2}$ peak was examined instead of the majority $3d_{5/2}$ peak, which partially overlaps with O 1s peak. As surface oxidation progresses, this overlap makes fitting of the Sb $3d_{5/2}$ oxide and sulfide components difficult and can lead to their overestimation.

Significantly, the Ga and As elemental spectra acquired after the acid-TAM passivation of GaSb and InAs, respectively, *do not*

Author's personal copy

resemble those obtained following similar treatments of GaAs [21,22]. This difference indicates that the TAM surface chemistry depends on the III–V compound, *not just the element*; hence, passivation results for a common element in two different III–V materials should not, in general, be assumed to be the same.

3.2. Quantitative analysis of passivation layers by XPS

The thickness and composition of passivation layers are calculated from the overlayer/bulk XPS intensity ratios as described previously [24] and are shown in Fig. 2 for each treatment as a function of time after passivation (solid bars for acid-TAM and hatched for base-TAM). Briefly, the thickness of the overlayer is calculated based on the ratio of the overlayer (oxide + sulfide) and bulk component intensities for a given element (taken from the integrated XPS peak areas) and the effective attenuation length (EAL). EAL values are calculated using NIST SRD-82 software, which takes into account material properties and kinetic energies of photoelectrons [24,31,32]. A representative series of Sb $3d_{3/2}$ peaks after acid-TAM treatment is presented in Fig. 3 and shows the evolution of the bulk, sulfide, and oxide peak components (Table 1) over time as the passivated sample is exposed to ambient conditions.

Each bar in Fig. 2 represents the total overlayer thickness; the light and dark portions of the bar indicate, respectively, the relative amounts of sulfide and oxide of a given element in the overlayer. For each material, two sets of values are calculated independently based on the spectra of group III and V elements. The thickness of each overlayer is thus probed by photoelectrons of two different kinetic energies (in Figs. 1 and 2, 2p photoelectrons are more surface sensitive than 3d photoelectrons) and the surface chemistry of each element is independently quantified.

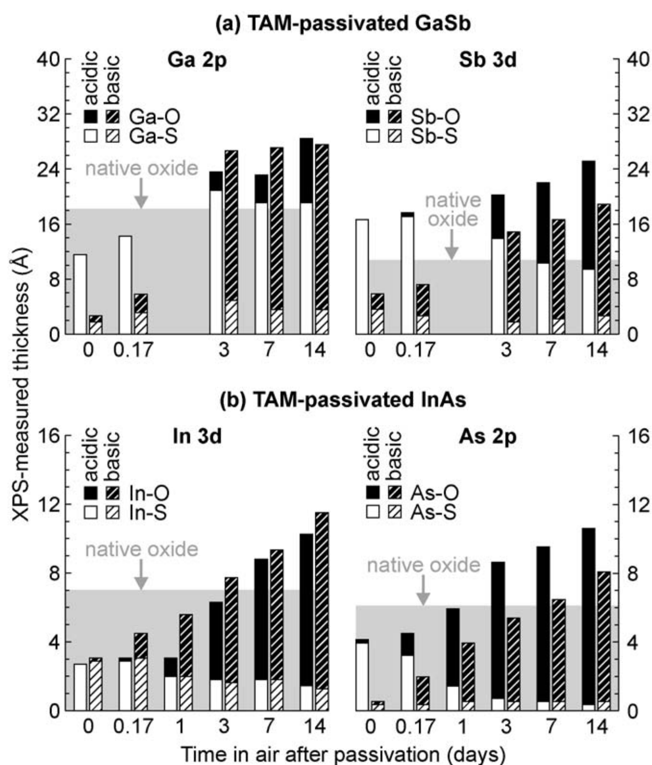

Fig. 2. Composition and thickness of overlayers on TAM-treated GaSb and InAs samples. The height of each bar represents the total thickness of an overlayer calculated from XPS data for GaSb (a) and InAs (b). The light (dark) portions of each bar indicate the relative amount of sulfide (oxide) of the specified elements in the overlayer. Solid and hatched bars, respectively, indicate treatments by acid- and base-activated TAM.

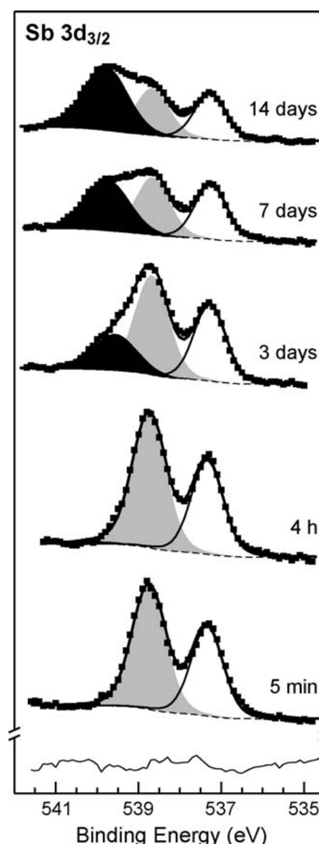

Fig. 3. Evolution of Sb 3d spectra on GaSb after acid-TAM passivation. For each spectrum, the length of exposure to ambient air after passivation is indicated. The fits illustrate the evolution of the three chemical components (Table 1): bulk Sb–Ga (thin line, no shading), sulfide Sb–S (gray shading), and oxide Sb–O (black shading). Symbols = data points; thick lines = overall fits; dashed lines = backgrounds; a representative fit residual is shown at the bottom of the panel.

3.3. Evolution of passivation layers in ambient air

On GaSb, the initial passivation layers produced by acid-TAM (≈16 Å) are thicker than those produced by base-TAM (≈6 Å); these thicker passivation layers correlate with slower reoxidation over the first three days (Fig. 2(a)). After acid-TAM passivation, no appreciable oxidation of GaSb occurs in the first four hours and significant oxidation begins only after about 3 days (Figs. 2(a) and 3). In contrast, the base-TAM passivated GaSb oxidizes significantly in the first 4 h and becomes comparable to an unpassivated control after 3 days. Overlayer thicknesses calculated from the Sb 3d and Ga 2p data exhibit the same trends (Fig. 2(a)); the systematically higher values derived from the more surface-sensitive Ga 2p data indicate that overlayers on GaSb are not uniform.

The apparent initial increase of the Ga–S thickness in Fig. 2(a) is actually a normalization artifact caused by the combination of the slower oxidation of Ga relative to Sb and the thickening of the overlayer during oxidation. During the first three days, the Ga–S bonds are largely left intact while Sb begins to oxidize. As detailed in Fig. 3, the increasing Sb oxidation thickens the combined sulfide/oxide overlayer, thus attenuating the intensity of signals from the bulk. A ratio of the approximately constant Ga–S component to the decreasing bulk Ga–Sb component produces the appearance in Fig. 2(a) of an increase in Ga–S at the surface. However, we find from a detailed examination of the absolute intensity of the Ga–S component that the amount of Ga–S gradually decreases with time, as expected.

Author's personal copy

On InAs, the main difference between the acid- and base-TAM passivation layers is in the presence and absence, respectively, of a significant As–S component, which results in a slightly thicker passivation layer immediately after the acid-TAM treatment (Fig. 2(b)). For the first 4 h, acid-TAM passivation offers better protection than does base-TAM. However, within 1 day after the acid-TAM passivation the As in the overlayer is already mostly oxidized. In contrast, the In component appears to oxidize at a slightly slower rate after the acid-TAM treatment than after base-TAM (Fig. 2(b)). This slower In oxidation occurs despite a comparable amount of In–S on both surfaces, and thus may be associated with the presence on the base-TAM surface of a small initial amount of In–O, which potentially nucleates faster oxidation.

3.4. Longevity of passivated, unpassivated, and untreated surfaces

Surprisingly, for both the acid- and base-TAM passivated surfaces the thicknesses of the reoxidation layers after 1 week were greater than the thicknesses of native oxide layers on respective *untreated*, as-grown surfaces (Fig. 2). This behavior might be caused by greater oxygen diffusion through the sulfide layers than through native oxides. Alternatively, we suspect that the As- or Sb-rich multilayer capping films (deposited at the termination of MBE growth) offer some degree of protection against oxygen diffusion, and that replacement of such layers with a thinner sulfide film—while offering better short-term passivation—ultimately allows a thicker oxide layer to grow when the sulfide layer is displaced.

The importance of the initial surface morphology and chemistry is also highlighted by the *unpassivated* InAs controls: made by stripping off the native oxide with ammonium hydroxide, they oxidized more slowly than similar surfaces etched in an acidic solution in our previous work [25]. We speculate that the mild stripping conditions used here resulted in InAs surfaces that were smoother and less reactive than surfaces produced by the harsher acid etching of InAs.

3.5. Surface chemistry of III–V semiconductors in pH-activated TAM solutions

The systematic data from this study combined with previous literature reports [15,16,18,21,22,24,33] indicate that treatments in solutions of inorganic and organic sulfides can produce a variety of passivation films on III–V semiconductors. Elucidating the underlying surface and solution chemistry, however, remains rather speculative, because only the final products of those reactions—passivated surfaces—can be readily analyzed by *ex-situ* methods.

For device passivation, treatment by thioacetamide solutions may offer several practical benefits compared to the more traditional treatments based on inorganic sulfides, such as $(NH_4)_2S_x$, which tend to etch III–V semiconductor surfaces more aggressively and leave sulfur residues. An additional advantage of TAM is the flexibility in the choice of the solution pH, which can be acidic or basic, in contrast to the intrinsically basic pH in aqueous solutions of inorganic sulfides. The unique chemical structure of TAM (Fig. 1(a)) is likely responsible for some of its special properties, as the adjacent sulfur and amine ligands provide multiple activation pathways in aqueous solutions. The absence of residues on TAM-passivated surfaces also suggests that, unlike aqueous sulfur ions, activated TAM molecules do not readily agglomerate in solution or on surfaces. Details of the TAM-passivation surface chemistry, however, remain uncertain, including the question of how TAM molecules partition upon surface adsorption.

The most surprising result of our comparative study is the variety of passivation films that can be produced by TAM treatments. While the pH-dependent differences in the thickness of sulfide films (Figs. 1–2) likely result from the interplay of the respective etching and reaction rates, the element- and compound-dependent chemistry is more difficult to rationalize. Nevertheless, our comparative data and individual results from previous studies clearly demonstrate that the passivation chemistry for a given Group III or V element depends not only on the element itself, but also on the specific III–V compound, e.g., Ga and As reactivities observed on GaAs surfaces [21,22] do not agree with the chemistry of the same two elements that we have measured on GaSb and InAs.

4. Conclusions

In conclusion, we have shown that the pH of aqueous solutions used for TAM passivation of GaSb and InAs significantly influences the resulting surface chemistry. Whereas base-TAM passivation produces a thin, self-limiting sulfide layer, acid-TAM passivation gives a much thicker sulfide film. Although the thicker sulfide layer produced by acid-TAM generally provides superior passivation for GaSb surfaces, on InAs it oxidizes more rapidly because of the apparent instability of As–S in air. In general, acid-TAM passivation offers good protection against oxidation for approximately one day. Because we have characterized these processes on both surfaces, we can recommend that acid-TAM treatment should be useful for passivating devices that will be used the same day, or for stabilizing the electronic properties of devices prior to capping them with a more robust protective film. For example, our preliminary results indicate that TAM passivation is compatible with subsequent encapsulation of devices in a polymer.

A somewhat unexpected and more general conclusion, suggested by our comparative studies and previous literature reports, is that the chemical effects of TAM treatments on Ga, Sb, In, and As depend not only on the individual element and reaction conditions, but also on the compound. In other words, the passivation chemistry for a common element in two different III–V materials should not, in general, be assumed to be the same.

Acknowledgements

The authors thank Drs. Brian Bennett and Chadwick Canedy (NRL) for growing the InAs and GaSb samples. D.Y.P. and R.S. thank Dr. Thomas Clark (NRL) for helpful discussions on the chemical properties of thioacetamide. R.S. acknowledges the support of an ASEE Postdoctoral Research Associateship. This work was funded by the Office of Naval Research and the Air Force Office of Scientific Research.

References

[1] S. Mou, J.V. Li, S.L. Chuang, J. Appl. Phys. 102 (2007) 066103.
[2] P.-Y. Delaunay, A. Hood, B.M. Nguyen, D. Hoffman, Y. Wei, M. Razeghi, Appl. Phys. Lett. 91 (2007) 091112.
[3] A. Hood, M. Razeghi, E.H. Aifer, G.J. Brown, Appl. Phys. Lett. 87 (2005) 151113.
[4] J.V. Li, S.L. Chuang, E.H. Aifer, E.M. Jackson, Appl. Phys. Lett. 90 (2007) 223503.
[5] E. Plis, S.J. Lee, Z. Zhu, A. Amtout, S. Krishna, IEEE J. Sel. Top. Quantum Electron. 12 (2006) 1269.
[6] L. Canali, J.W.G. Wildoer, O. Kerkhof, L.P. Kouwenhoven, Appl. Phys. A 66 (1998) S113.
[7] A.J.A. Salesse, P. Calas, J. Nieto, F. Chevrier, Y. Cuminal, G.P. Ferblantier, Phys. Status Solidi C 4 (2007) 1508.
[8] M. Mehta, G. Balakrishnan, S. Huang, A. Khoshakhlagh, A. Jallipalli, P. Patel, M.N. Kutty, L.R. Dawson, D.L. Huffaker, Appl. Phys. Lett. 89 (2006) 211110.
[9] M.R. Kitchin, M. Jaros, Physica E 18 (2003) 498.
[10] M. Walther, G. Weimann, Phys. Status Solidi A 203 (2006) 3545.
[11] Z.M. Zhu, P. Bhattacharya, E. Plis, X.H. Su, S. Krishna, J. Phys. D: Appl. Phys. 39 (2006) 4997.
[12] Y. Zhang, N. Baruch, W.I. Wang, Appl. Phys. Lett. 63 (1993) 1068.

Author's personal copy

[13] J. Katz, Y. Zhang, W.I. Wang, Appl. Phys. Lett. 62 (1993) 609.
[14] D.L. Smith, C. Mailhiot, J. Appl. Phys. 62 (1987) 2545.
[15] Y. Fukuda, S. Ichikawa, M. Shimomura, N. Sanada, Y. Suzuki, Vacuum 67 (2002) 37.
[16] Y. Fukuda, Y. Suzuki, N. Sanada, M. Shimomura, S. Masuda, Phys. Rev. B 56 (1997) 1084.
[17] S. Ichikawa, N. Sanada, N. Utsumi, Y. Fukuda, J. Appl. Phys. 84 (1998) 3658.
[18] Z.Y. Liu, T.F. Kuech, D.A. Saulys, Appl. Phys. Lett. 83 (2003) 2587.
[19] M.J. Lowe, T.D. Veal, C.F. McConville, G.R. Bell, S. Tsukamoto, N. Koguchi, J. Cryst. Growth 237–239 (2002) 196.
[20] M.J. Lowe, T.D. Veal, C.F. McConville, G.R. Bell, S. Tsukamoto, N. Koguchi, Surf. Sci. 523 (2003) 179.
[21] E.D. Lu, F.P. Zhang, S.H. Xu, X.J. Yu, P.S. Xu, Z.F. Han, F.Q. Xu, X.Y. Zhang, Appl. Phys. Lett. 69 (1996) 2282.
[22] F.Q. Xu, E.D. Lu, H.B. Pan, C.K. Xie, P.S. Xu, X.Y. Zhang, Surf. Rev. Lett. 8 (2001) 19.
[23] D.Y. Petrovykh, M.J. Yang, L.J. Whitman, Surf. Sci. 523 (2003) 231.
[24] D.Y. Petrovykh, J.M. Sullivan, L.J. Whitman, Surf. Interface Anal. 37 (2005) 989.
[25] D.Y. Petrovykh, J.P. Long, L.J. Whitman, Appl. Phys. Lett. 86 (2005) 242105.
[26] E. Papis, A. Kudla, T.T. Piotrowski, K. Golaszewska, E. Kaminska, A. Piotrowska, Mater. Sci. Semicond. Process. 4 (2001) 293.
[27] M.S. Carpenter, M.R. Melloch, M.S. Lundstrom, S.P. Tobin, Appl. Phys. Lett. 52 (1988) 2157.
[28] J.F. Fan, H. Oigawa, Y. Nannichi, Jpn. J. Appl. Phys. 27 (1988) L1331.
[29] C.J. Sandroff, R.N. Nottenburg, J.C. Bischoff, R. Bhat, Appl. Phys. Lett. 51 (1987) 33.
[30] K. Moller, L. Toben, Z. Kollonitsch, C. Giesen, M. Heuken, F. Willig, T. Hannappel, Appl. Surf. Sci. 242 (2005) 392.
[31] A. Jablonski, C.J. Powell, Surf. Sci. Rep. 47 (2002) 35.
[32] C.J. Powell, A. Jablonski, NIST Electron Effective-Attenuation-Length Database, Version 1.0 (SRD-82)., US Department of Commerce, National Institute of Standards and Technology, Gaithersburg MD, 2001.
[33] Y. Nannichi, J.F. Fan, H. Oigawa, A. Koma, Jpn. J. Appl. Phys. 27 (1988) L2367.